The EMBO Journal vol.14 no.22 pp.5467–5475, 1995

Monitoring dynamic changes in free Ca^{2+} concentration in the endoplasmic reticulum of intact cells

Mayte Montero, Marisa Brini, Robert Marsault, Javier Alvarez, Roberto Sitia[1], Tullio Pozzan and Rosario Rizzuto[2]

Department of Biomedical Sciences and CNR Center for the Study of Mitochondrial Physiology, University of Padova, Padova and [1]Department of Biological and Technological Research (DIBIT), Milano, Italy

[2]Corresponding author

Direct monitoring of the free Ca^{2+} concentration in the lumen of the endoplasmic reticulum (ER) is an important but still unsolved experimental problem. We have shown that a Ca^{2+}-sensitive photoprotein, aequorin, can be addressed to defined subcellular compartments by adding the appropriate targeting sequences. By engineering a new aequorin chimera with reduced Ca^{2+} affinity, retained in the ER lumen via interaction of its N-terminus with the endogenous resident protein BiP, we show here that, after emptying the ER, Ca^{2+} is rapidly re-accumulated up to concentrations of >100 μM, thus consuming most of the reporter photoprotein. An estimate of the steady-state Ca^{2+} concentration was obtained using Sr^{2+}, a well-known Ca^{2+} surrogate which elicits a significantly slower rate of aequorin consumption. Under conditions in which the rate and extent of Sr^{2+} accumulation in the ER closely mimick those of Ca^{2+}, the steady-state mean lumenal Sr^{2+} concentration ($[Sr^{2+}]_{er}$) was ~2 mM. Receptor stimulation causes, in a few seconds, a 3-fold decrease of the $[Sr^{2+}]_{er}$, whereas specific inhibition of the ER Ca^{2+} ATPase leads to an ~10-fold drop in a few minutes.

Keywords: calcium/endoplasmic reticulum/photoprotein(s)/signal transduction/targeting

Introduction

Fluorescent indicators (Tsien *et al.*, 1982) and photoproteins (Ashley and Ridgway, 1968) have been used in the last two decades to monitor Ca^{2+} concentration in living cells. While the indicators can be loaded into cells either via intracellularly trappable esters or by microinjection, until recently only the latter technique could be employed with Ca^{2+}-sensitive photoproteins. However, thanks to the cloning of the cDNA encoding the photoprotein aequorin, the time-consuming and traumatic procedure of microinjection can be now be replaced by the simpler technique of cDNA transfection. This latter approach, i.e. the modification of the aequorin cDNA with the insertion of targeting sequences and thus the specific subcellular localization of the photoprotein has provided another important opportunity in the study of Ca^{2+} homeostasis. In this way, we have constructed aequorin chimeras targeted to the mitochondrial matrix (Rizzuto *et al.*, 1992), nucleus (Brini *et al.*, 1993) and cytosol (Brini *et al.*, 1995) of living cells, which have provided new and often unexpected information on Ca^{2+} homeostasis in intact cells.

The targeting of aequorin or the fluorescent Ca^{2+} indicators to the lumen of the endoplasmic reticulum (ER) has also been attempted by various groups. However, several problems have arisen. In the case of fluorescent dyes, trapping within the ER is not specific, and identification of the loaded structures is very often impossible. Moreover, in the ER lumen, Ca^{2+} dyes appear to be saturated with Ca^{2+} (Glennon *et al.*, 1992) and/or, as in the case of lower affinity indicators such as Mag–fura-2 (Hofer and Machen, 1993), Mag–indo-1 (Tse *et al.*, 1994) or furaptra (Hirose and Iino, 1994), to have such a poor selectivity over Mg^{2+} that calibration is highly uncertain. This notwithstanding, an estimate of the free Ca^{2+} concentration in the ER lumen could be obtained, which was, at rest, in the range 60–200 μM (Tse *et al.*, 1994; Hofer *et al.*, 1995). Different problems have plagued the approach of targeting Ca^{2+}-sensitive photoproteins to the ER. Appending a Lys-Asp-Glu-Leu (KDEL) motif to the C-terminus of the photoprotein allows ER targeting (Kendall *et al.*, 1992a, 1994) but causes a spontaneous, Ca^{2+}-independent degradation (Nomura *et al.*, 1991; Watkins and Campbell, 1993). The signal of ER-targeted aequorin, although quite difficult to calibrate, apparently indicated a mean Ca^{2+} concentration in the order of 1–5 μM (Kendall *et al.*, 1992a). This value not only appears much lower than that measured with the fluorescent indicators, but also is difficult to reconcile with the known affinities of ER Ca^{2+} binding proteins and with the kinetic characteristics of the ER Ca^{2+} channels and pumps.

We here describe the use of an aequorin chimera targeted to the ER employing a new strategy which allows for the specific localization of the recombinant protein to the ER lumen without modifying its critical C-terminal proline. We show that not only a normal aequorin moiety but also a low-affinity aequorin (generated by the point mutation of one of the three Ca^{2+} binding sites) is endowed with a Ca^{2+} affinity which is too high to reliably measure the concentration of this cation in the ER lumen. By taking advantage of Sr^{2+}, a divalent cation which is transported by Ca^{2+} ATPases and permeates through Ca^{2+} channels but elicits a slower rate of photoprotein consumption than Ca^{2+} itself, we demonstrate that divalent cation homeostasis in this endomembrane system can be followed quantitatively in intact cells both under resting conditions and upon cell stimulation. We conclude that the Ca^{2+} concentration in the ER lumen under resting conditions is ~2–3 mM, and drops very rapidly upon the receptor-

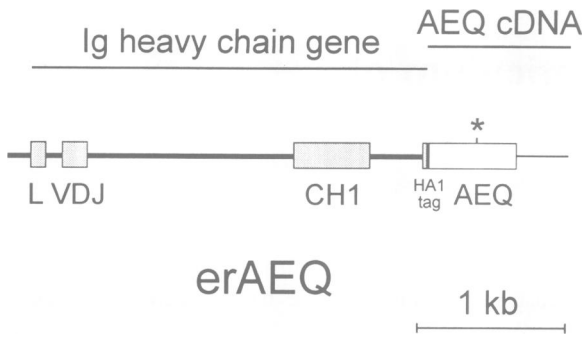

Fig. 1. Schematic map of the chimeric erAEQ cDNA. In the Ig moiety (on the left), shaded boxes and thick lines indicate coding and intronic regions, respectively; in the aequorin portion, the coding and non-coding regions of the cDNA are indicated by a white box and a thin line, respectively. The short sequence encoding the HA1 tag, located upstream of the aequorin moiety, is indicated by a black box. An asterisk shows the position of the single amino acid substitution of erAEQmut (Asp119→Ala), which decreases the affinity of aequorin.

induced production of inositol triphosphate (IP_3). Taken together, these results are of major importance not only for the understanding of Ca^{2+} homeostasis, but in general for a better comprehension of ER physiology.

Results

Figure 1 shows the structure of the chimeric cDNA. The encoded polypeptide (erAEQ) includes the leader sequence (L), the VDJ and C_H1 domains of an Igγ2b heavy chain (HC; Sitia *et al.*, 1990), and aequorin (Inouye *et al.*, 1985) at the C-terminus. In this chimera, retention in the ER should depend not on the typical C-terminal sequence KDEL (Pelham, 1989), but on the presence at the N-terminus of aequorin of the C_H1 domain. This domain is known to interact with the lumenal ER protein BiP, thus causing the retention of the Ig HC in the lumen. In plasma cells, the interaction is displaced by the light chain (LC), while in any other cells a chimeric polypeptide including the C_H1 domain of the HC is expected to be selectively retained in the ER (Sitia *et al.*, 1990, and references therein).

The photoprotein domain was also modified by introducing an epitope tag (Field *et al.*, 1988) and a point mutation (Asp119→Ala), which reduce the Ca^{2+} affinity of the photoprotein (Kendall *et al.*, 1992b). The latter modification appeared necessary because aequorin is well suited for measuring $[Ca^{2+}]$ between 0.1 and 10.0 μM (Blinks *et al.*, 1978b), whereas the $[Ca^{2+}]_{er}$ was expected to be much higher (Pozzan *et al.*, 1994). The shift in Ca^{2+} affinity is clearly apparent from the *in vitro* calibration (Figure 2). Interestingly, because of the cooperativity between the three Ca^{2+} binding sites of aequorin, the mutation, which affects the second EF-hand domain, changed the slope of the curve. The range of aequorin sensitivity can be expanded further by employing divalent cations other than Ca^{2+} (Blinks *et al.*, 1978a). We utilized Sr^{2+}, which is known to be a suitable Ca^{2+} surrogate (Somlyo and Somlyo, 1971); Sr^{2+} permeates across Ca^{2+} channels (Bezprozvanny and Ehrlich, 1994) and is actively transported, although with a lower affinity, by both the plasma membrane and the sarco-endoplasmic Ca^{2+} ATPases (SERCAs; Fleschner and Kraus-Friedmann,

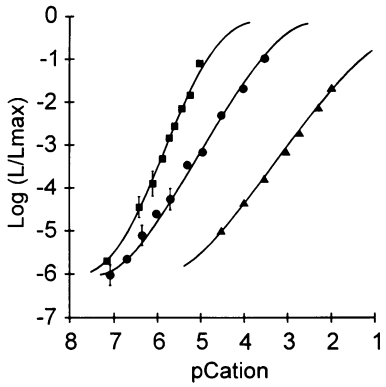

Fig. 2. Determination of the Ca^{2+} and Sr^{2+} affinities of the erAEQ chimeras. (■) Ca^{2+} response curve of the erAEQ chimera including the wild-type aequorin cDNA (erAEQwt); the Ca^{2+} affinity of this chimera is virtually identical to that of native aequorin (results not shown). (●) Ca^{2+} response curve of the erAEQ chimera including the Asp119→Ala mutation (erAEQmut). (▲) Sr^{2+} response curve of erAEQmut. Each data point is the average of at least five different trials. The standard deviation, when significant, is shown. pCation, $-\log[cation^{2+}]$; *L*, rate of photon emission immediately after mixing the cell lysate with the Ca^{2+} (or Sr^{2+}) buffer; L_{max}, integral of counts from the mixing to the end of the experiment (i.e. after aequorin consumption with excess $cation^{2+}$). For the calibration curve, the supernatant of a lysate of HeLa cells expressing erAEQwt or erAEQmut was employed, and the $cation^{2+}$ affinity of the recombinant photoprotein was measured as described in Materials and methods.

1986; Holguin, 1986; Horiuti, 1986). As shown for the ER-targeted aequorin chimera with low Ca^{2+} affinity (erAEQmut) in Figure 2, the calibration curve of aequorin for Sr^{2+} is similar in slope to that for Ca^{2+}, but shifted to the right. Altogether, by combining the two approaches, an aequorin-based ER probe can measure $[cation^{2+}]$ ranging from the μM to the mM range.

The chimeric cDNA, inserted in the expression vector pcDNAI (Invitrogen), was employed successfully both in transient expression experiments and in generating clones that stably express the chimeric photoprotein. To verify the effectiveness of the retention strategy, the release of erAEQmut in the culture medium of a transfected clone was measured. On average, ~0.1%/h of total erAEQmut was released in the medium, confirming that indeed the photoprotein is mostly retained intracellularly. As for the intracellular localization, Figure 3 compares the immunofluorescence staining of the ER endogenous marker ERp72 (Figure 3A; Haugejorden *et al.*, 1991) with that of erAEQmut (Figure 3B) in transiently transfected, doubly stained HeLa cells. It is apparent that the staining, which in the former case obviously labels all the cells, shows a very similar distribution and pattern; the high magnification of a cell expressing erAEQmut (Figure 3C) clearly shows the delicate reticular pattern typical of the ER.

Native aequorin is composed of an apoprotein and a covalently bound coenzyme, coelenterazine. To utilize recombinant aequorin as a Ca^{2+} indicator, the holoprotein must be reconstituted, and this is accomplished by incubating the cells with the membrane-permeant prosthetic group coelenterazine (Rizzuto *et al.*, 1994a,b, 1995). However, after a standard incubation with coelenterazine, i.e. in culture medium containing ~2 mM Ca^{2+}, the total number of photons obtained with an erAEQmut-expressing clone was very low ($<10^5$ c.p.s./coverslip, results not shown;

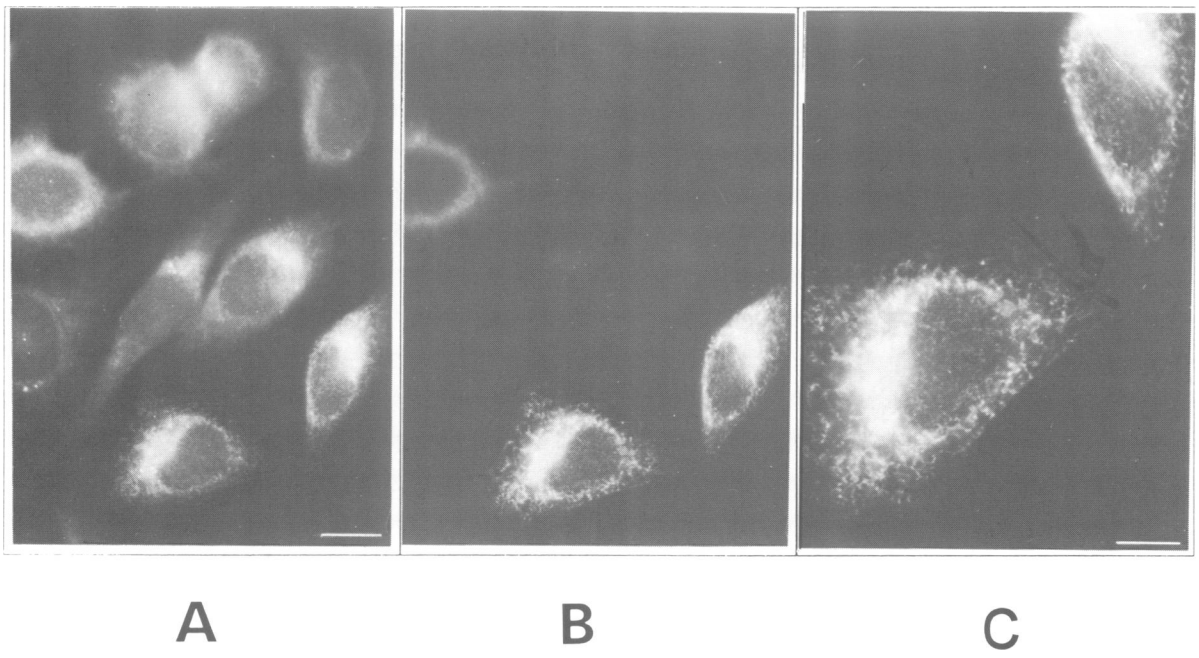

Fig. 3. Immunolocalization of the ER marker ERp72 and erAEQmut in transiently transfected HeLa cells. Double staining with polyclonal anti-Erp72 (**A**) and monoclonal anti-HA1 (**B**) antibodies, revealed by FITC-labeled anti-rabbit and TRITC-labeled secondary antibodies. In (**C**), a higher magnification of the erAEQmut immunostaining is shown. Immunocytochemistry was performed as described in Materials and methods. Transiently transfected cells were employed for this experiment because, when compared with stable clones, a higher level of expression (and thus a stronger signal) was observed in the positive cells. However, the same staining pattern was also obtained with the clones (data not shown). (A and B) Bar 17 μm; (C) bar 9 μm.

compared with $>10^6$ c.p.s. of clones transfected with mitochondrially targeted aequorin and showing a comparable intensity of immunocytochemical staining). A similar, low level of reconstitution was observed under these conditions in other clones expressing erAEQmut or erAEQwt, or in transiently transfected cells with either construct. This result was not entirely surprising, because $[Ca^{2+}]_{er}$ was predicted to be very high, and thus aequorin consumption was expected to effectively compete with reconstitution. *In vitro*, we have observed (data not shown) that at $[Ca^{2+}]$ >50 μM, little or no net reconstitution takes place. In fact, at these high $[Ca^{2+}]$ values, as soon as coelenterazine binds to the apoprotein, the probability of photon emission, and thus consumption, becomes very high. If this is the case for the ER, little or no functional aequorin should be expected in intact cells.

To verify whether the poor reconstitution *in vivo* was indeed caused by the high $[Ca^{2+}]$ of the ER lumen, we reconstituted apoaequorin after the depletion of $[Ca^{2+}]_{er}$ by ionophores and SERCA inhibitors (Figure 4). Following this treatment, the immunostaining of erAEQmut was not modified (results not shown), while a dramatic increase was observed in the count yield ($>10^6$ c.p.s./coverslip, i.e. ~20-fold more than the controls). Figure 4B shows the kinetics of aequorin photon emission in intact cells after reconstitution under the latter conditions. The signal, close to background in EGTA-containing medium, showed a dramatic transient increase (which consumed ~90% of total aequorin) upon $CaCl_2$ addition; the final addition of digitonin resulted in a marginal emission of photons. The calibration of the luminescent signal into $[Ca^{2+}]_{er}$ values (Figure 4C) shows that the apparent average $[Ca^{2+}]_{er}$ increased from a resting value of ~1 μM to a peak of ~150 μM. After the peak, $[Ca^{2+}]_{er}$ dropped very rapidly to a slowly declining plateau of ~10 μM. The corresponding data for cytosolic Ca^{2+} concentration ($[Ca^{2+}]_c$), as measured in parallel with fura-2, are shown in Figure 4A. Unlike the $[Ca^{2+}]_{er}$, upon the addition of Ca^{2+} to the perfusing medium, the $[Ca^{2+}]$ in the cytosol increased rapidly from a very low value (~10 nM) to a steady-state level of ~100–150 nM, without any obvious gross overshoot above this concentration. The $[Ca^{2+}]_c$ of cells maintained and loaded with fura-2 in Ca^{2+} medium was indistinguishable from that reached after 2–3 min by cells undergoing the depletion protocol (results not shown). Several explanations can be offered for the unexpected transient and very large overshoot of $[Ca^{2+}]_{er}$ described in Figure 4C (see Discussion). Among these, a heterogeneity of the $[Ca^{2+}]_{er}$ or the presence of a small fraction of erAEQmut in a post-ER compartment could easily explain the experimental data. In particular, if the bulk ER was endowed with a $[Ca^{2+}]$ >100 μM, while a subfraction (or a post-ER compartment) had a lumenal $[Ca^{2+}]$ of ~10 μM, the first would consume all its aequorin in a few seconds and the latter much more slowly. The average signal would thus reflect initially the high $[Ca^{2+}]$ regions; after the consumption of aequorin in those areas, the average signal would reflect the regions of low $[Ca^{2+}]$.

To test this possibility, we took advantage of the much lower affinity of aequorin for Sr^{2+}. As discussed above, Sr^{2+} is the only known divalent cation which, in addition to triggering aequorin luminescence and permeating through Ca^{2+} channels, is also effectively transported by Ca^{2+} ATPases. If, after the Ca^{2+} depletion protocol, 1 mM Sr^{2+} was added to the medium, $[Sr^{2+}]_c$ increased to ~1.1 μM (Figure 4D). The kinetics of $[Sr^{2+}]_c$ increase were very similar to those of Ca^{2+} (compare Figure 4D with A). Figure 4E and F shows the kinetics of aequorin light

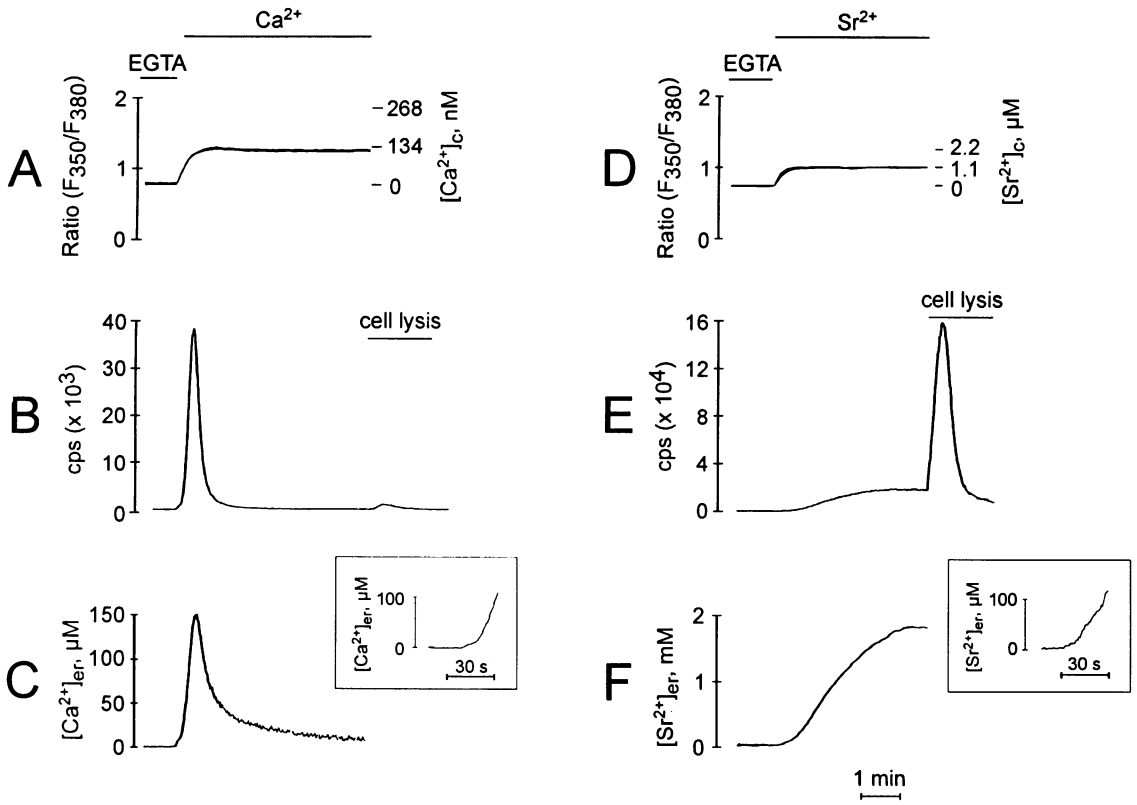

Fig. 4. Kinetics of $[cation^{2+}]_c$ and $[cation^{2+}]_{er}$ increase upon the readdition of Ca^{2+} and Sr^{2+} to Ca^{2+}-depleted cells. The experiments shown here and in the following figure were performed utilizing a HeLa cell clone (EM26), stably transfected with erAEQmut. Similar results were obtained utilizing other erAEQmut expressing clones or HeLa cells transiently transfected with the erAEQmut expression plasmid. The upper traces (**A** and **D**) show the $[cation^{2+}]_c$ measurements with fura-2. The middle (**B** and **E**) and lower (**C** and **F**) traces show, respectively, erAEQmut light emission and the conversion of erAEQmut luminescence data into $[cation^{2+}]$ values. (C) and (F) include an inset showing, at the same scale, the initial phase of the increase in $[cation^{2+}]_{er}$. In all experiments, $[Ca^{2+}]_{er}$ was first reduced with a typical Ca^{2+} depletion protocol, as described in Materials and methods. (A)–(C) and (D)–(F) correspond to the kinetics of refilling with 1 mM Ca^{2+} and Sr^{2+}, respectively. At the end of the aequorin experiments, to estimate the total photoprotein content, unconsumed aequorin was discharged ('cell lysis') by perfusing the cells with a hypotonic Ca^{2+}-rich solution, as described previously (Rizzuto *et al.*, 1994a). These and the following data are typical of at least five independent experiments, which gave the same results.

emission and the calculated $[Sr^{2+}]_{er}$, respectively, in a parallel batch of cells under the same conditions. As expected, the rate of photon emission upon Sr^{2+} addition was much lower than that with Ca^{2+} (~30% of total aequorin was consumed in 5 min compared with ~90% over the same time period with Ca^{2+}). Comparison of the calibrated $[Ca^{2+}]_{er}$ and $[Sr^{2+}]_{er}$ traces (Figure 4C and F) indicates that the uptake in the ER was, for the two cations, sigmoidal and had virtually identical initial rates (6.7 ± 0.4 and 6.3 ± 0.4 µM/s for Ca^{2+} and Sr^{2+}, respectively; see insets in Figure 4C and F). However, ER Ca^{2+} accumulation apparently ceased after 10–20 s, while that of Sr^{2+} continued to increase for 2–3 min and then reached a steady state. Overall, $[Sr^{2+}]_{er}$, when compared with $[Ca^{2+}]_{er}$, showed a much larger increase, up to a plateau value of ~2 mM. According to the hypothesis discussed above, the drop in $[Ca^{2+}]_{er}$ would be apparent only in the high $[Ca^{2+}]$ compartment and caused by the rapid consumption of aequorin.

The question then arises as to whether the steady-state concentrations reached in the ER by Sr^{2+} closely reflect those of Ca^{2+}. Obviously, this extrapolation rests on a series of assumptions. In particular, as for other organelles, the steady-state $[cation^{2+}]$ is expected to be the result of an equilibrium between the uptake of the cation via the SERCA and leakage into the cytosol. The former depends on the affinity of the pump(s) and on the cytosolic concentration of the cation, and the latter on the passive permeability of the membrane and on the intralumenal $[cation^{2+}]$. In order for the two cations, Ca^{2+} and Sr^{2+}, to be accumulated in the ER lumen up to the same final concentration, it is thus necessary that the rates of accumulation and leakage are similar for both cations. As far as accumulation is concerned, the affinity of SERCAs for Sr^{2+} is known to be about one order of magnitude lower than that for Ca^{2+} (Holguin, 1986; Horiuti, 1986), while the V_{max} for the two cations is the same (Fleschner and Kraus-Friedmann, 1986). Thus under our experimental conditions, at the steady state, the rate of Sr^{2+} accumulation is expected to be very similar to that of Ca^{2+} because $[Sr^{2+}]_c$ is ~10-fold higher than $[Ca^{2+}]_c$. Direct information on the leakage rate was sought in an experiment (results are shown in Figure 5A) which measures *in situ* the passive diffusion of Ca^{2+} and Sr^{2+} into the ER. To this end, after reconstituting erAEQmut with the protocol described above, cells were permeabilized with digitonin, thereby exposing the ER to the perfusion medium under conditions of complete inhibition of active transport (by treatment with inhibitors of $cation^{2+}$ accumulation and ATP synthesis). The passive leakage was initiated by

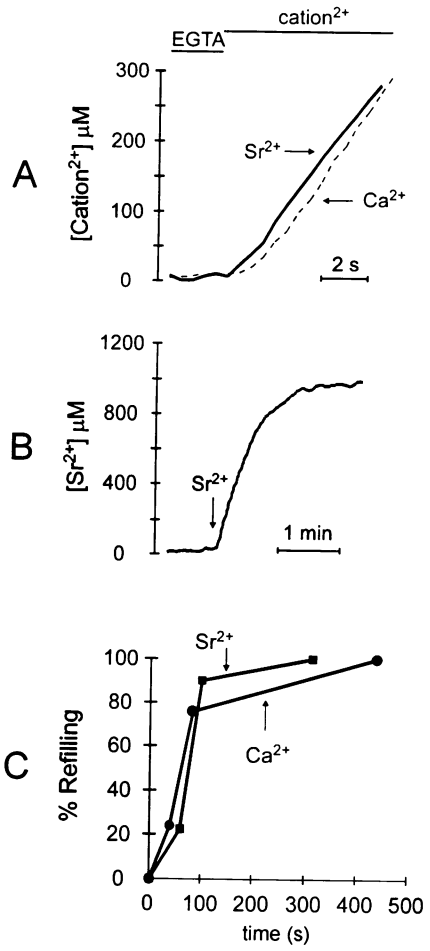

Fig. 5. Rates of Ca^{2+} and Sr^{2+} leakage into the ER in permeabilized cells, and the time course of ER refilling with the two cations in intact cells. (**A**) Initial phase of passive Ca^{2+} and Sr^{2+} leakage into the ER lumen in cells permeabilized with digitonin. To avoid any active uptake, the cells were treated with inhibitors of SERCAs (1 µM thapsigargin and 10 µM tBuBHQ) and of mitochondrial ATP production (1 µg/ml oligomycin and 1 µg/ml antimycin). The experiments were performed at 22°C. The cells were initially permeabilized with 100 µM digitonin in KRB containing 0.1 mM EGTA. After 3 min, digitonin was removed and perfusion continued for another 3 min in KRB + EGTA. Where indicated, the perfusion medium contained 1 mM $CaCl_2$ or 1 mM $SrCl_2$ in place of EGTA. (**B**) Time course of ER refilling with Sr^{2+} by passive leakage in permeabilized cells. Conditions were as in (A), but measurement was prolonged until equilibrium was reached. (**C**) Time course of ER refilling with Ca^{2+} and Sr^{2+} in intact cells, as revealed by the amplitudes of agonist-induced $[Ca^{2+}]_c$ or $[Sr^{2+}]_c$ peaks. After the ER depletion protocol and loading with fura-2, 1 mM Ca^{2+} or Sr^{2+} was added to the incubation medium. At different times, 3 mM EGTA were added, followed immediately by 100 µM histamine. Fura-2 measurements were performed as described in Materials and methods. In the graph, the amplitude of the $[Ca^{2+}]_c$ and $[Sr^{2+}]_c$ peaks was normalized to the maximal response (i.e. that observed 15 min after cation readdition). No difference in the amplitude of the $[Ca^{2+}]_c$ peak was observed between control cells which did not undergo the depletion/refilling protocol and cells refilled for 15 min. A very similar graph was obtained when the rates of $cation^{2+}$ release were plotted instead of the amplitudes of the $[cation^{2+}]_c$ peaks.

perfusing the permeabilized cells with saline solutions containing 1 mM Ca^{2+} or Sr^{2+}; the leakage rate into the ER, which was derived from the rate of increase of $[Ca^{2+}]_{er}$ and $[Sr^{2+}]_{er}$, was very similar for the two cations. Again, the rate of Ca^{2+} accumulation could be followed for only a few seconds, because afterwards, as a result of rapid aequorin exhaustion, calibration became highly inaccurate. In the case of Sr^{2+}, a steady-state concentration was reached which corresponded closely to the $[Sr^{2+}]$ of the perfusing medium; the good match between the expected value and the calibrated signal (Figure 5B) indicates that inside the ER the sensitivity of aequorin to $[Sr^{2+}]$ is similar to that measured *in vitro*.

Based on these data, the time course of Ca^{2+} and Sr^{2+} refilling of the ER can be expected to be similar. This is confirmed by the experimental results displayed in Figure 5C, which show the amplitudes and rates (results not shown) of histamine-induced $[Ca^{2+}]_c$ and $[Sr^{2+}]_c$ peaks (expressed as a percentage of the maximal response) at different times upon re-exposing the cells to external Ca^{2+} or Sr^{2+} after the ER depletion protocol. It is apparent that the increases in the $[Ca^{2+}]_c$ and $[Sr^{2+}]_c$ responses have an almost identical time course, thus indicating a similar speed of refilling of the ER with the two cations.

After refilling the ER with Sr^{2+}, the effects on $[Sr^{2+}]_c$ and $[Sr^{2+}]_{er}$ of 2,5-di(tert-butyl)-1,4-benzohydroquinone (tBuBHQ; Kass *et al.*, 1989), an inhibitor of the SERCAs, and histamine, an agonist coupled to IP_3 generation (Bootman *et al.*, 1992), were analyzed (Figure 6). tBuBHQ caused a slow rise of $[Sr^{2+}]_c$ (2.5 µM at the peak; Figure 6A), paralleled by a very large decrease in $[Sr^{2+}]_{er}$ (Figure 6B) which reached a value of ~200 µM in ~3 min (corresponding to an aequorin light output close to basal values). Conversely, the receptor agonist, which caused a large increase in $[Sr^{2+}]_c$ (Figure 6C), induced a rapid drop in $[Sr^{2+}]_{er}$ (half-time 5 s), which stabilized at 0.7 mM throughout the stimulation (Figure 6D); a further decrease in $[Sr^{2+}]_{er}$ was obtained upon addition of the SERCA inhibitor. These data indicate that agonist stimulation causes either a diffuse, partial emptying of the ER lumen or a complete release, limited, however, to an IP_3-sensitive portion of the organelle.

Discussion

Measuring $[Ca^{2+}]_{er}$ quantitatively and kinetically is a difficult, but important, task which may allow us to address major questions in cell biology. Indeed, not only is the ER, or some of its subcompartments, believed to be the main Ca^{2+} store of non-muscle cells, functioning as a rapidly mobilizable reservoir of Ca^{2+} released into the cytosol upon stimulation of the plasma membrane receptors, but the Ca^{2+} content of the ER is also known to affect protein synthesis, sorting and degradation which occur in this organelle (for a review see Sitia and Meldolesi, 1992). In addition, several lines of evidence indicate that $[Ca^{2+}]$ in the lumen of the ER controls the Ca^{2+} permeability of the plasma membrane by modulating, probably via the release into the cytosol of a second messenger, the activity of specific Ca^{2+} channels (Fasolato *et al.*, 1994). However, despite this large amount of interest, the information about ER Ca^{2+} handling is still fragmentary. The total Ca^{2+} content has been measured in several direct or indirect ways, and there is a general agreement that it amounts to several mmol/l of ER volume (for a review see Pozzan *et al.*, 1994). In contrast, there is much discrepancy between the reported estimates of lumenal free $[Ca^{2+}]$ (Kendall *et al.*, 1992a; Tse *et al.*, 1994; Hofer *et al.*, 1995). The reason for these discrepan-

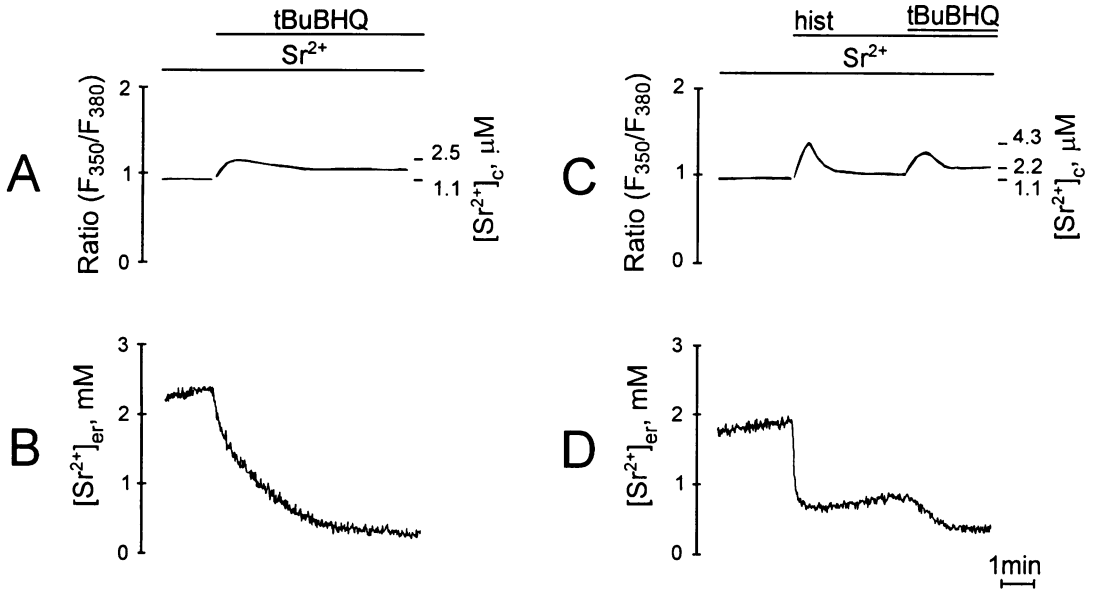

Fig. 6. Effects of histamine and the Ca^{2+} ATPase inhibitor tBuBHQ on $[Sr^{2+}]_c$ and $[Sr^{2+}]_{er}$. The upper (**A** and **C**) and lower traces (**B** and **D**) show the monitoring of $[Sr^{2+}]_c$ and $[Sr^{2+}]_{er}$ in EM26 cells with fura-2 and erAEQmut, respectively. Prior to recording, ER was refilled with Sr^{2+} as in Figure 4. Where indicated, the cells were treated with 10 µM tBuBHQ and/or 100 µM histamine (hist). Reconstitution of the photoprotein, collection and calibration of the luminescence signal, as well as all other experimental conditions, were as described in Materials and methods. The $[Sr^{2+}]_c$ increases induced by histamine or SERCA blockers in EM26 cells were not significantly different from those observed in clones expressing low amounts of erAEQ or in control cells, thus suggesting that the expression of erAEQ does not affect the cation^{2+} buffering capacity of the ER lumen.

cies appears to be most probably methodological. Fluorescent Ca^{2+} indicators, when applied as hydrolyzable esters, have been reported to load, at least in some cell types, into the ER. However, a closer examination of the data reveals that such trapping of the indicator is not specific to the ER, because other organelles, such as mitochondria, lysosomes and secretory granules, also sequester the dyes. Thus, to a best approximation, the values obtained with the indicators are the means of several intracellular organelles. Unsurprisingly, Tse *et al.* (1994) reported that the apparent $[Ca^{2+}]_{er}$ in gonadotropes is in part affected by mitochondrial poisons. A further complication in this approach is the need to somehow eliminate the strong cytosolic signal, by permeabilization, dialysis or selective quenching (Glennon *et al.*, 1992; Tse *et al.*, 1994; Hofer *et al.*, 1995).

On the other hand, targeting a Ca^{2+}-sensitive photoprotein to the ER lumen, although largely overcoming the problem of selective localization of the indicator, has been affected by other problems. In particular, the obvious strategy, i.e. adding a KDEL C-terminal sequence to ensure ER retention, drastically altered the aequorin luminescence properties (Nomura *et al.*, 1991; Watkins and Campbell, 1993). Indeed, the apparent $[Ca^{2+}]_{er}$ calculated by this method is surprisingly at least one order of magnitude lower than that measured recently with the Ca^{2+} dyes. The ER-targeted aequorin chimera developed here includes several features which proved useful for the specific analysis of $[Ca^{2+}]_{er}$, such as (i) the targeting strategy does not affect the luminescence properties of aequorin, (ii) the HA1 epitope allows a straightforward subcellular localization, and (iii) the single amino acid substitution in the aequorin sequence, which decreases its Ca^{2+} affinity, allows the chimera to reliably report higher Ca^{2+} concentrations, thus expanding the pCa range that can be explored with the recombinant photoprotein.

As to the effectiveness of the ER retention strategy, the minute release of the photoprotein into the medium despite the strong expression, and the immunostaining pattern clearly indicate that the vast majority of the aequorin chimera is retained in the ER lumen. Of course, it is very difficult to exclude the possibility that a minor subfraction of the aequorin pool is localized in other vesicular structures, such as the Golgi apparatus or secretory vesicles (see below).

However, despite the low Ca^{2+} affinity of our construct when reconstitution was carried out under standard conditions, a very low total luminescence signal was obtained, suggesting that, at the physiological Ca^{2+} content of the ER, reconstitution is counteracted by a high rate of aequorin discharge. The alternative possibility, i.e. the existence in the ER lumen of factors other than Ca^{2+} preventing the optimal reconstitution of the luminescent protein, is ruled out by the demonstration that Ca^{2+} depletion with ionophores and/or inhibitors of the SERCAs is sufficient to increase drastically the reconstitution efficiency.

In the latter conditions, the apparent behavior of $[Ca^{2+}]_{er}$ upon the readdition of Ca^{2+} to the medium was quite unexpected. In particular, in a few seconds it reached ~100 µM, followed by a precipitous decrease to <10 µM. We considered various possibilities: (i) slow buffering in the ER lumen; (ii) rapid inactivation of the uptake; (iii) activation of a leakage pathway; and (iv) artefacts caused by the intrinsic characteristics of the aequorin signal. The last possibility appears the most likely. In fact, slow buffering is incompatible with the known kinetic constants of the ER Ca^{2+} binding proteins (K_{on} very fast), while the rapid inhibition of uptake or the activation of leakage is inconsistent with the kinetics of net Ca^{2+} uptake observed in both isolated ER vesicles and permeabilized cells. More importantly, the first three hypotheses appear to be incompatible with the kinetics of Ca^{2+} refilling

presented in Figure 5. If indeed the free lumenal $[Ca^{2+}]$ reached a peak after 15–20 s and then dropped to about one-tenth of its maximal value in the steady state, one would predict that the rate (and extent) of agonist-induced Ca^{2+} release should be maximal at the peak of $[Ca^{2+}]_{er}$ and then slow down when $[Ca^{2+}]_{er}$ apparently decreased to the lower steady-state value. This is clearly not the case. On the contrary, data indicate that the $[Ca^{2+}]_{er}$ gradually increases and reaches a steady state in ~2–3 min. Accordingly, the decrease in $[Ca^{2+}]_{er}$ is thus only apparent. Two not mutually exclusive possibilities were considered as an explanation for this artefactual calibration of the aequorin signal. Firstly, as mentioned in Results, if only a minor fraction of aequorin (e.g. 10%) was contained in a compartment (of the ER or of another organelle) with a low $[Ca^{2+}]$, while the rest of the aequorin (90%) was exposed to a high $[Ca^{2+}]$, the overall kinetics of aequorin photon emission would indeed mimic those observed experimentally. In particular, a fast rate of light emission would be observed immediately after the addition of Ca^{2+} to the medium; in a few seconds, however, the aequorin content in the high Ca^{2+} compartment would drop drastically and, although the fractional rate of aequorin consumption would continue to increase, the absolute rate of photon emission would diminish drastically and eventually become negligible. However, at the same time, the relatively small signal coming from the compartment with low $[Ca^{2+}]$, negligible at the beginning, would remain relatively constant with time; thus, upon exhaustion of the large aequorin pool of the compartment with high $[Ca^{2+}]$, it would represent the only source of photon emission. Were this the case, the calibration procedure would give the false impression of a mean $[Ca^{2+}]_{er}$ increasing rapidly and then eventually stabilizing at a low level. We have mimicked this model mathematically and demonstrated that it is possible to fit the experimental data almost perfectly, assuming that 90% of aequorin is contained in a compartment which in steady state reaches 3 mM Ca^{2+}, and 10% in a compartment which reaches 10 μM Ca^{2+} (results not shown). However, an alternative explanation is also possible: the luminescence kinetics could also be nicely fitted by another model in which the aequorin is all contained in a high Ca^{2+} environment, provided that a small continuous reconstitution of aequorin takes place as a result of the presence of some coelenterazine (after the washout from the medium) inside the cells.

However, whichever model is correct, it is obvious that not even the mutated aequorin is suited to monitoring the high $[Ca^{2+}]$ in the ER lumen. On the other hand, the use of Sr^{2+} as a Ca^{2+} surrogate allows a reliable measurement of the steady-state $[Sr^{2+}]_{er}$, but is itself subject to criticisms. Our data, however, strongly support the notion that the values of $[Sr^{2+}]_{er}$ closely mimic those of $[Ca^{2+}]_{er}$. In particular, given that the SERCAs have a lower affinity for Sr^{2+} than for Ca^{2+} (about one order of magnitude), it is predicted that the same net rate of cation uptake into the ER would be reached only if the cytosolic concentrations of the two cations were different, and in particular if $[Sr^{2+}]_{er}$ was 10-fold higher than $[Ca^{2+}]_{er}$. This is indeed the case in our experiments. For the same rate of cation uptake, the steady-state free cation concentration in the ER lumen would be the same only if the rates of leakage were the same. This latter condition was verified experimentally, although admittedly it could be measured directly only in permeabilized cells.

A final simple consideration argues strongly in favor of the conclusion that indeed the Ca^{2+} concentration in the ER lumen should not be very different from that of Sr^{2+}. It has been shown that the rate of Ca^{2+} efflux through IP_3 receptors is, within the range 10 μM–3 mM, linearly dependent on $[cation^{2+}]$ on the lumenal side (Bezprozvanny and Ehrlich, 1994). The rate of Ca^{2+} release induced by histamine added 20 s after initiation of the Ca^{2+} refilling protocol is ~20 times slower than that measured at steady state (Figure 5). Given that after 20 s the $[Ca^{2+}]_{er}$ is ~100 μM, it immediately derives that at steady state the $[Ca^{2+}]_{er}$ should be ~20-fold higher, i.e. ~2 mM, similar to the measured $[Sr^{2+}]_{er}$.

In conclusion, altogether the data presented here demonstrate that under resting conditions, Sr^{2+} (and thus presumably Ca^{2+}) is accumulated in the lumen of the bulk ER up to the millimolar range, and is rapidly released by IP_3-generating agonists and SERCA blockers. The mean $[cation^{2+}]_{er}$ values measured (in the mM range) here are much higher than those suggested previously, not only using chimeric ER aequorin (i.e. in the low μM range; Kendall *et al.*, 1992a), but also using fluorescent Ca^{2+} indicators (60–200 μM; Tse *et al.*, 1994; Hofer *et al.*, 1995), and are in full agreement with the known affinities and kinetic properties of SERCAs, Ca^{2+} binding proteins and Ca^{2+} release channels. This information, together with a tool for specifically monitoring the lumenal $[cation^{2+}]$, will now allow us to address directly, in intact cells, a number of key biological questions, such as the role of the ER Ca^{2+} in modulating the activity of Ca^{2+} channels and pumps and in controlling specific organelle functions, e.g. protein sorting.

Materials and methods

Site-specific mutagenesis of the aequorin cDNA

The HA1-tagged aequorin cDNA (Brini *et al.*, 1995) was mutagenized to introduce the Asp119→Ala mutation using the Pharmacia kit based on the unique site elimination procedure (Deng and Nickoloff, 1992), according to the supplier's protocols. The following primer was used to mutate the aequorin cDNA: 5′-GCTCCATTTTGGGCTTTGTCGACG-ATA-3′ (antisense), corresponding to the sequence 5′-TATC(Ile)GTC-(Val)GAC(Asp)AAA(Lys)G**CC**(**Ala**)CAA(Gln)AAT(Asn)GGA(Gly)-GC-3′ (sense). Specifically, codon 119 was changed from GAT to GCC, thus mutating Asp119 of the encoded polypeptide to Ala, and a silent mutation was introduced in codon 116 (GTT→GTC), thus creating a new *Sal*I site, useful for the rapid screening of mutated cDNAs.

Construction of the ER-targeted aequorin chimeras

The start point for the construction was plasmid pSV–Vγ2b/μtp (Sitia *et al.*, 1990), which includes a complete Igγ2b heavy gene and thus allows the recombinant expression of the Ig HC in plasma cells. In a first step, the wild-type aequorin cDNA was inserted at a unique *Xho*I site located at the beginning of the sequence encoding the C_H2 domain. For this purpose, suitable *Xho*I sites were inserted upstream and downstream of the aequorin *Hin*dIII–*Eco*RI fragment through cloning steps in the appropriate vectors. Using this approach, five spurious amino acids were inserted between the Ig and aequorin coding sequences. The chimeric cDNA was transfected in NSO cells (a plasma cell line not expressing the LC; Sitia *et al.*, 1990) and evidence was obtained of the ER localization of the recombinant protein (results not shown). The final construct was then prepared. A *Sal*I site was generated by PCR at the 5′ end of the Ig coding region, which was utilized for subcloning the whole construct (erAEQ, shown schematically in Figure 1) into the cloning vector pBSK$^+$ (Stratagene). At this stage, the *Hin*dIII–*Eco*RI fragment of the wild-type aequorin cDNA (Inouye *et al.*, 1985) was

substituted with the corresponding fragment of HA1-tagged 'normal' (Brini *et al.*, 1995) or 'low-affinity' (see above) aequorin, thus generating the chimeras denoted erAEQwt and erAEQmut, respectively. The chimeric cDNAs were subcloned in the mammalian expression vector pcDNAI (Invitrogen) and utilized in the transfection experiments.

Cell culture and transfection

HeLa cells were grown in Dulbecco's modified Eagle's medium (DMEM), supplemented with 10% fetal calf serum (FCS), in 75 cm^2 Falcon flasks. In transient expression experiments, the cells were seeded onto 13 mm glass coverslips and allowed to grow to 50% confluence. At this stage, transfection with erAEQwt or erAEQmut (2–4 μg DNA/coverslip) was carried out as described previously (Rizzuto *et al.*, 1994b), and aequorin measurements or immunocytochemistry were performed 36 h after transfection. For generating cell clones stably expressing erAEQmut, a 10 cm dish of HeLa cells was transfected with 36 μg of erAEQmut/pcDNAI and 4 μg of pSV2neo (Southern and Berg, 1982). Selection was carried out with 0.8 mg/ml G418, as described elsewhere (Rizzuto *et al.*, 1994b, 1995). In all, 50 clones were isolated and tested for aequorin expression by measuring the Ca^{2+}-dependent light emission of coelenterazine-reconstituted cell lysates. Among the selected clones, erAEQmut expression (as estimated by a comparison with known amounts of purified protein) ranged between 5 and 70 ng/mg protein. Clone EM26 was the highest producer, and was employed in the experiments presented here, although similar data were obtained using other clones.

In vitro calibration of erAEQwt and erAEQmut

The calibration curve of erAEQwt and erAEQmut, presented in Figure 2, was determined *in vitro* by exposing lysates of cell clones stably expressing the recombinant photoprotein to solutions containing 110 mM KCl, 10 mM NaCl, 1 mM free Mg^{2+}, 40 mM HEPES, pH 7.0 at 22°C, 5 mM EGTA (or HEDTA) and known concentrations of Ca^{2+} or Sr^{2+}. The procedure for fitting the curve to the experimental data, and other details, are described in Brini *et al.* (1995).

Ca^{2+} measurements with aequorin and fura-2

EM26 cells were plated onto 13 mm round coverslips (for the aequorin experiments) or 20×8 mm rectangular coverslips (for the fura-2 experiments). As discussed in the text, before reconstituting aequorin, $[Ca^{2+}]_{er}$ was reduced using the following protocol. Cells were incubated for 5 min with the Ca^{2+} ionophore A23187 (10 μM) and the SERCA inhibitor tBuBHQ (10 μM) in KRB (Krebs–Ringer modified buffer: 125 mM NaCl, 5 mM KCl, 1 mM Na_3PO_4, 1 mM $MgSO_4$, 5.5 mM glucose, 20 mM HEPES, pH 7.4, 37°C), supplemented with 3 mM EGTA, followed by washing in KRB containing 0.1 mM EGTA, 5% bovine serum albumin and 10 μM tBuBHQ. Similar results were obtained when $[Ca^{2+}]_{er}$ was reduced with different protocols (e.g. omitting tBuBHQ from the protocol described above, or repetitively stimulating the cells with histamine in EGTA-containing medium in the presence of tBuBHQ). Aequorin reconstitution was then carried out by incubating the cells with 5 μM coelenterazine for 1 h in KRB containing 100 μM EGTA and 10 μM tBuBHQ. In the fura-2 measurements, prior to recording, the cells were incubated for 30 min with 5 μM fura-2/AM. In the erAEQmut measurements, fura-2 loading was omitted because we observed no effect of fura-2 on $[cation^{2+}]_{er}$ dynamics (results not shown). All experiments were performed in KRB medium, supplemented, where indicated, with 0.1 mM EGTA, 1 mM $CaCl_2$ or $SrCl_2$. In the fura-2 measurements, the coverslip was transferred to the cuvette of a multi-wavelength fluorimeter (Cairn Research Ltd, Sittingbourne, UK; excitation 350 and 380 nm, emission 500 nm); the fura-2 signal was calibrated as described elsewhere (Rizzuto *et al.*, 1993). In the erAEQmut measurements, the coverslip with the cells was introduced into the perfusion chamber of a purpose-built luminometer (Cobbold and Lee, 1991; Rizzuto *et al.*, 1995). Aequorin light emission was measured as described previously (Rizzuto *et al.*, 1994a), and calibrated using a computer algorithm (Brini *et al.*, 1995) and the Ca^{2+} and Sr^{2+} affinity constants measured *in vitro*.

Immunolocalization of the HA1-tagged recombinant photoprotein

At 48 h after transfection, HeLa cells were processed for immunofluorescence as follows. The cells were fixed with 3.7% formaldehyde in PBS for 20 min, washed two or three times with PBS and then incubated for 10 min in PBS supplemented with 50 mM NH_4Cl. Permeabilization of cell membranes was obtained with a 5 min incubation with 0.1% Triton X-100 in PBS, followed by a 30 min wash with 0.2% gelatin (type IV, from calf skin) in PBS. The cells were then incubated for 1 h at 37°C in a wet chamber with a 1:200 dilution (in PBS) of the monoclonal antibody 12CA5 (initially a kind gift from J.Pouyssegur, Nice, France; then obtained from BAbCo, Berkeley, CA), which recognizes the HA1 tag (Field *et al.*, 1988), and then with a 1:100 dilution of the rabbit polyclonal antibody ERp72(C) (Haugejorden *et al.*, 1991) raised against the 16 C-terminal residues of the ER resident protein Erp72. Staining was then carried out with fluorescein isothiocyanate (FITC)-labeled anti-rabbit and tetramethylrhodamine (TRITC)-labeled anti-mouse secondary antibodies. After each antibody incubation, the cells were washed four times with PBS. Fluorescence was then analyzed with a Zeiss Axioplan microscope and photographed using Kodak Ektachrome 200 ASA film.

Acknowledgements

We thank C.Bastianutto for carrying out some of the experiments, G.Ronconi and M.Santato for technical assistance, Y.Sakaki for the wild-type aequorin cDNA, J.Pouyssegur for the anti-HA1 antibody, M.Green and J.Bergeron for the anti-ERp72 antibody, Y.Kishi for coelenterazine, and P.Cobbold for help in constructing the aequorin detection system. This work was supported by grants from the Italian Research Council (CNR) 'ACRO' project, from 'Telethon', from the Italian Association for Cancer Research (AIRC), from the 'AIDS project' of the Italian Health Ministry, from Human Frontiers (RG-520/95M), from the Italian Ministry of University and Scientific Research and from the British Research Council to T.P. and R.R. M.M., R.M. and J.A. are recipients of EEC 'Human Capital and Mobility' fellowships.

References

Ashley,C.C. and Ridgway,E.B. (1968) *Nature*, **219**, 1168–1169.
Bezprozvanny,I. and Ehrlich,B.E. (1994) *J. Gen. Physiol.*, **104**, 821–856.
Blinks,J.R., Allen,D.G., Prendergast,F.G. and Harrer,G.C. (1978a) *Life Sci.*, **22**, 1237–1244.
Blinks,J.R., Mattingly,P.H., Jewell,B.R., vanLeewen,M., Marrer,G.C. and Allen,D. (1978b) *Methods Enzymol.*, **57**, 292–328.
Bootman,M.D., Berridge,M.J. and Taylor,C.W. (1992) *Am. J. Physiol.*, **450**, 163–178.
Brini,M., Murgia,M., Pasti,L., Picard,D., Pozzan,T. and Rizzuto,R. (1993) *EMBO J.*, **12**, 4813–4819.
Brini,M., Marsault,R., Bastianutto,C., Alvarez,J., Pozzan,T. and Rizzuto,R. (1995) *J. Biol. Chem.*, **270**, 9896–9903.
Cobbold,P.H. and Lee,J.A.C. (1991) In McCormack,J.G. and Cobbold,P.H. (eds), *Cellular Calcium. A Practical Approach*. Oxford University Press, Oxford, UK, pp. 55–81.
Deng,W.P. and Nickoloff,J.A. (1992) *Anal. Biochem.*, **200**, 81–88.
Fasolato,C., Innocenti,B. and Pozzan,T. (1994) *Trends Pharmacol. Sci.*, **15**, 77–83.
Field,J., Nikawa,J., Broeck,D., MacDonald,B., Rodgers,L., Wilson,I.A., Lerner,R.A. and Wigler,M. (1988) *Mol. Cell. Biol.*, **8**, 2159–2165.
Fleschner,C.R. and Kraus-Friedmann,N. (1986) *Eur. J. Biochem.*, **154**, 313–320.
Glennon,M.C., Bird,G.S., Takemura,O., Thastrup,O. and Putney,J.W. (1992) *J. Biol. Chem.*, **267**, 25568–25575.
Haugejorden,S.M., Srinivasan,M. and Green,M. (1991) *J. Biol. Chem.*, **266**, 6015–6018.
Hirose,K. and Iino,M. (1994) *Nature*, **372**, 791–794.
Hofer,A.M. and Machen,T.E. (1993) *Proc. Natl Acad. Sci. USA*, **90**, 2598–2602.
Hofer,A.M., Schlue,W.-R., Curci,S. and Machen,T.E. (1995) *FASEB J.*, **9**, 788–798.
Holguin,J.A. (1986) *Arch. Biochem. Biophys.*, **251**, 9–16.
Horiuti,K. (1986) *Am. J. Physiol.*, **373**, 1–23.
Inouye,S., Noguchi,M., Sakaki,Y., Takagi,Y., Miyata,T., Iwanaga,S., Miyata,T. and Tsuji,F.I. (1985) *Proc. Natl Acad. Sci. USA*, **82**, 3154–3158.
Kass,G.E.N., Duddy,S.K., Moore,G.A. and Orrenius,S.A. (1989) *J. Biol. Chem.*, **264**, 15192–15198.
Kendall,J.M., Dormer,R.L. and Campbell,A.K. (1992a) *Biochem. Biophys. Res. Commun.*, **189**, 1008–1016.
Kendall,J.M., Sala-Newby,G., Ghalaut,V., Dormer,R.L. and Campbell, A.K. (1992b) *Biochem. Biophys. Res. Commun.*, **187**, 1091–1097.
Kendall,J.M., Badminton,M.N., Dormer,R.L. and Campbell,A.K. (1994) *Anal. Biochem.*, **221**, 173–181.
Nomura,M., Inouye,S., Ohmiya,Y. and Tsuji,F.I. (1991) *FEBS Lett.*, **295**, 63–66.

Pelham,H.R.B. (1989) *Annu. Rev. Cell Biol.*, **5**, 1–23.
Pozzan,T., Rizzuto,R., Volpe,P. and Meldolesi,J. (1994) *Physiol. Rev.*, **74**, 595–636.
Rizzuto,R., Simpson,A.W.M., Brini,M. and Pozzan,T. (1992) *Nature*, **358**, 325–328.
Rizzuto,R., Brini,M., Murgia,M. and Pozzan,T. (1993) *Science*, **262**, 744–747.
Rizzuto,R., Bastianutto,C., Brini,M., Murgia,M. and Pozzan,T. (1994a) *J. Cell Biol.*, **126**, 1183–1194.
Rizzuto,R., Brini,M. and Pozzan,T. (1994b) *Methods Cell Biol.*, **40**, 339–358.
Rizzuto,R., Brini,M., Bastianutto,C., Marsault,R. and Pozzan,T. (1995) *Methods Enzymol.*, **260**, 417–428.
Sitia,R. and Meldolesi,J. (1992) *Mol. Biol. Cell*, **3**, 1067–1072.
Sitia,R., Neuberger,M., Alberini,C., Bet,P., Fra,A., Valetti,C., Williams,G. and Milstein,C. (1990) *Cell*, **60**, 781–790.
Somlyo,A.V. and Somlyo,A.P. (1971) *Science*, **174**, 955–958.
Southern,P.J. and Berg,P. (1982) *J. Mol. Appl. Genet.*, **1**, 327–341.
Tse,F.W., Tse,A. and Hille,B. (1994) *Proc. Natl Acad. Sci. USA*, **91**, 9750–9754.
Tsien,R.Y., Pozzan,T. and Rink,T.J. (1982) *J. Cell Biol.*, **94**, 325–334.
Watkins,N.J. and Campbell,A.K. (1993) *Biochem. J.*, **293**, 181–185.

Received on June 20, 1995; revised on August 4, 1995